Bull. Astr. Soc. India (2004) **32**, 283–294

Intensities of CII and CO lines and emissions from interstellar dust

Abdul Qaiyum
Department of Physics, A.M.U., Aligarh 202002, India

Received 21 June 2004; accepted 1 September 2004

Abstract. A comparative study of Weingartner and Draine (2001) (hereinafter referred as WD) and Bakes and Tielens (1994) (hereinafter referred as BT) models of photoelectric heating efficiencies of gas shows that for neutral medium WD model of photoelectric heating dominates over the BT model but in a medium where grains are positively charged BT is higher by many factors as compared to WD. WD model predicts a maximum photoelectric heating efficiency of the gas $\epsilon \sim 0.029$ and a maximum line intensity ratio of [CII] emission to that of total FIR emission $\sim 2.5 \times 10^{-2}$. Ingalls et al. (2002) and Juvela et al. (2003) observed almost the same values for ϵ and intensity ratios for high latitude clouds. Intensity of interstellar radiation field G_0 is estimated from the observed line intensities of CII and CO emissions for number of galactic and extragalactic photodissociation regions. It is found that G_0 is highly correlated with the observed intensity of FIR with an intercept equal to 1.23×10^{-4} (ergs $cm^{-2}s^{-1}sr^{-1}$), which is almost same as the ISRF of Habing (1968). This shows that ISRF photons absorbed by the dust grains are reradiated fully in the near -IR and far -IR.

Keywords : IR and near-IR - heating - cooling - CO and CII lines- ISRF

1. Introduction

The structure of the interstellar medium depends to a large extent on the processing of interstellar radiation field (ISRF) by the dust grains. FUV radiation in the energy range $5 < h\nu < 13.6$ eV ionizes dust grains, and a fraction $\epsilon < 0.03$ of the available energy is converted into gas heating (Juvela et al. 2003; WD 2001; BT 1994). The gas cools down after radiating its energy at millimeter and submillimeter wavelengths through the fine

structure transitions from the neutral and ionized elements (carbon, oxygen, silicon and iron) and rotational transitions (J→J-1) of CO, which is the most abundant molecule in the interior of the medium. Hence, the interstellar gas and ISRF are well coupled. Direct coupling of the non-ionizing photons to neutral gas is, however, difficult due to its low gas opacity. Instead, the dust will absorb most of these photons, and the absorbed energy will be reradiated in the near and far-infrared (FIR). Therefore, one expects a connection between G_0 (the intensity of ISRF in units of Habing (1968)) and CII(158μm) and CO (2.6mm) line emissions from the photoelectric heated gas and FIR emissions from dust grains.

Wolfire et al. (1989) have shown that CII(158μm) line intensity (I_{CII}), CO($J = 1 \rightarrow 0$) line intensity (I_{CO}) and FIR continuum intensity (I_{FIR}) from dust grains towards number of photodissociation regions associated with HII regions, planetary nebulae and reflection nebulae of galactic and extragalactic medium are correlated to a large extent. Large scale survey of COBE (Cosmic Background Explorer) satellite using FIRAS (Far Infrared Absolute Spectrometer) and DIRBE (Diffuse Infrared Background Spectrometer) revealed a link between the CII and FIR emission properties of the cold neutral medium. Ingalls et al. (2002) examined [CII] and FIR emissions towards a sample of translucent clouds using ISO (Infrared Space Observatory) and found that $I_{CII}/I_{FIR} \sim 2.5 \times 10^{-2}$. Juvela et al. (2003) concluded that the observed ratio I_{CII}/I_{FIR} is remarkably constant for high latitude clouds (HLCs).

In the recent years, it has become abundantly clear that photoelectric heating efficiency is a sensitive function of the distribution of dust and their sizes and associated grain charging, realistic photon yields and electron sticking coefficients. BT have provided photoelectric heating model for interstellar medium, where heating is considered mainly due to the polycyclic aromatic hydrocarbons (PAHs) and graphite of sizes $< 10^2$ Å. WD have proposed a number of heating rates under a variety of conditions based on the model of Li and Draine (2001) in which the smallest grains are PAHs, the largest consists of graphite, and grains of intermediate size have optical properties intermediate between those of PAHs and graphite. Silicate grains are also considered.

In view of this development we examine the photoelectric heating rates of BT and WD and its impact on the photoelectrically heated gas emitting CII(158μm), CO(2.6 mm) and far-IR line and continuum. Photoelectric heating rates and the fraction of heat energy radiated away due to fine structure transition of [CII] are plotted in Figures 1-3. The maximum value of ϵ is ~ 0.029 (Fig. 2) obtained from WD, which is almost the same as observed by Juvela et al. (2003). The maximum value of calculated intensity ratio $I_{CII}/I_{FIR} \sim 2.5 \times 10^{-2}$ (Fig. 3) which is almost the same as deduced by Ingalls et al. (2002) for HLCs.

The observations of CII(158 μm) and CO (2.6 mm) line intensities (I_{CII} and I_{CO}) and integrated FIR intensities I_{FIR} (in units of ergs cm^{-2} sec^{-1} sr^{-1}) towards a number of photodissociation regions associated with HII regions, planetary nebulae, and reflection

nebulae of galactic and extragalactic medium are taken from Wolfire et al. (1989) and Crawford et al. (1985). The calculations for the line intensities ((I_{CII} and I_{CO}) for all the sources have been performed using the escape probability formalism of Qaiyum and Ali (2003). FUV radiation field G_0, number density of total hydrogen (neutral hydrogen and hydrogen molecule) N (cm^{-3}) and velocity field (Doppler width) parametrs of the clouds are estimated through the best fit of the observed intensity. Calculated and observed intensities are compared in Figure 4 and the number densities of hydrogen are plotted in Figure 5 for the said models. The estimated parameters of line emitting regions are presented in Table 1.

The value of G_0 obtained from the observed intensity ratio I_{CII}/I_{CO} is a measure of intensity in units of Habing (1968). The observed intensity of infrared radiation for each source is plotted against G_0 in Figure 6. The slope of the curve obtained is interestingly equal to the average ISRF of Habing (1968). This shows ISRF is strongly coupled with infrared radiation intensity I_{FIR}.

2. Photoelectric heating rates and line emissions

The structure of the interstellar medium depends to a large extent on the heating and cooling processes of the interstellar gas. It has now been established that in diffuse and dense interstellar clouds ($A_v \leq 2$) the gas is mainly heated by photoelectrons expelled from dust grains by FUV radiations (de Jong 1977; Draine 1978; BT; WD). Such UV illuminated regions, generally associated with HII regions, planetary nebulae, reflection nebulae, and normal and active galactic nuclei are dominantly cooled by fine structure lines of [CI], [CII], [OI], [SiII] and [FeII], and rotational transitions of CO molecule. Hence, line emissions from such regions are coupled with the FUV radiation field. Therefore, a model calculation of photoelectric heating rate by FUV photons and cooling due to fine structure and rotational transitions can result in an estimate of G_0.

In order to calculate photoelectric heating rate consistent with the observations, photoemission processes and associated grain charging, realistic photon yields, distribution of photoelectron kinetic energies and electron sticking coefficients are very important under different interstellar conditions. All the parameters depend on the grain size, composition of grain and charging state as well as the spectrum of the illuminating radiation. BT and WD have discussed all the aspects in great detail. BT have given a formula for photoelectric heating rates, while WD have proposed a set of formulae based on the dust model of Li and Draine (2001), which is claimed to be valid under variety of conditions.

For the purpose of calculation of heating rates and loss of radiation, radiative transfer equation is solved at each position in the cloud. We adopt one dimensional plane parallel geometry in which FUV radiation field illuminates one side of the cloud and it is attenuated as exp(-$k_\lambda A_v$) provided that total visual extinction is large. The values k_λ range from ~ 1 to 3.5. The R_v=A_v/E_{B-V}, ratio of visual extinction to reddening is taken as 3.1.

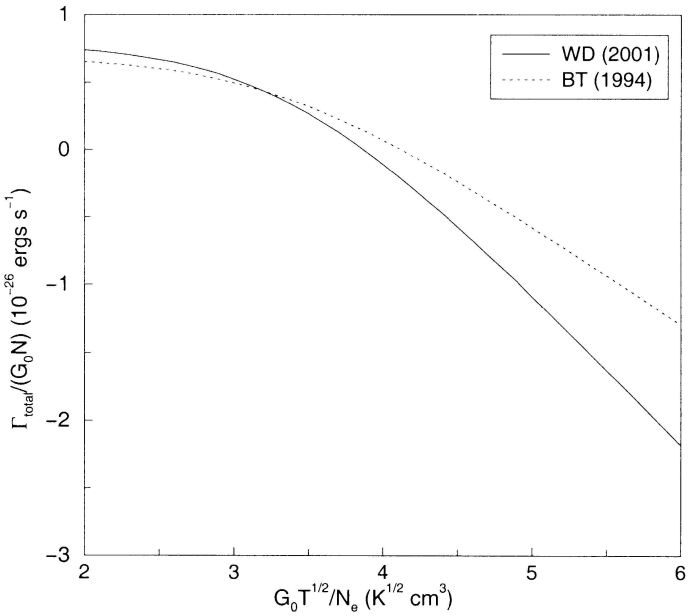

Figure 1. The photoelectric heating rate Γ_{total} per hydrogen density for average interstellar radiation field of Habing (1968).

The standard relationship between hydrogen column density N_H and visual extinction A_v is adopted as N_H=1.87 $\times$ $10^{21}A_v$ (Bohlin, Savage and Drake 1978). The abundance of PAHs is taken as 6×10^{-5} (Li and Draine 2001). For the purpose of determination of chemical and thermal structure of the medium a chemical and thermal balance is set up at each position of the source. The interstellar chemical network contains a set of 12 elements (H, He, C, N, O, Na, Mg, Si, P, S, Cl and Fe) and about 100 species of organic and inorganic molecules. The physical processes and their reaction rates are taken from Qaiyum (2003).

The amount of energy required to expel electrons from the surface of the grains by FUV photons is $I_p = W + (Z + 1)e^2/a$. For carbonaceous and silicate grains the work function W is 4.4 and 8 eV respectively. Z is the charge on the surface of grain and a is its radius. Thus energy available to the ejected electron to be shared by the gas is $(h\nu - I_p)$. In cold neutral medium, the grains too are neutral due, to which I_p is very close to W and the expelled electrons from the neutral grain carry large amount of energy, which is deposited in the medium. Therefore, the photoelectric heating efficiency for neutral medium is optimal. Contrary to that, when the grains are positively charged, the fraction of energy carried by the ejected electron is reduced, resulting in decrease of photoelectric heating efficiency.

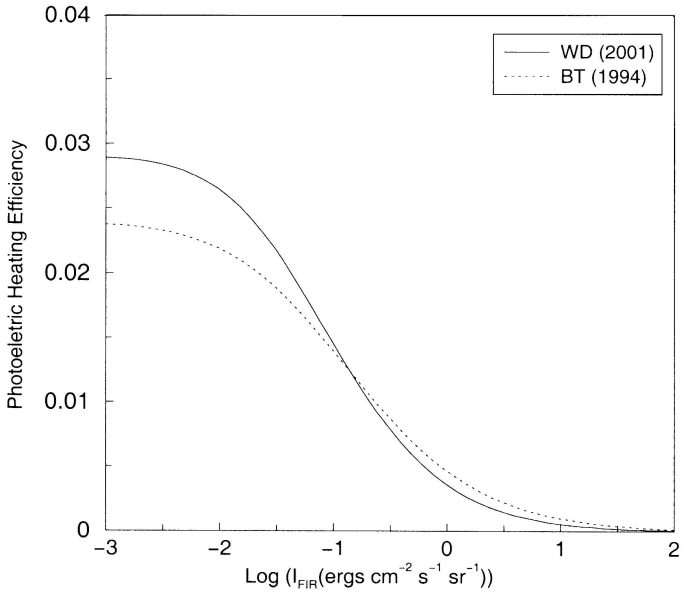

Figure 2. Photoelectric heating efficiency at $N = 10^4$ (cm^{-3}).

The photoelectric heating rates Γ_{total}/G_0N for ISRF of Habing (1968) in a range $10^2 \leq G_0\sqrt{T}/N_e \leq 10^6$ (K$^{1/2}$ cm^3) for WD and BT models are plotted in Figure 1. From the figure it is clear that for $G_0\sqrt{T}/N_e \leq 10^3$ (i.e. neutral medium) photoelectric heating rate due to WD is slightly higher than BT. Contrary to that for the medium $G_0\sqrt{T}/N_e \geq 10^3$ (where grains are positively charged) the photoelectric heating rate due to BT is higher by number of factors. On two counts WD and BT models differ. Firstly, the electron attachment coefficient, which governs the neutralization of the grain, used by BT are larger by many factors than that used by WD. Secondly, WD have included silicate grains in addition to small and large grain of PAHs and graphite (a>100Å), while BT considered only PAHs and graphite grains up to $a \leq 10^2$Å. When grains are neutral i.e. $G_0\sqrt{T}/N_e \leq 10^3$, sticking coefficient plays no role, photoelectric heating rate due to WD is higher because of consideration of large number of grains. When grains are positively charged (i.e. $G_0\sqrt{T}/N_e \geq 10^3$) BT dominates over WD due to high sticking coefficient of electron (S_e).

Although bulk of the FUV flux is absorbed by the grains and reradiated as infrared continuum, a fraction ϵ termed as photoelectric heating efficiency (the ratio between the kinetic energy of photons available to heat the gas and FUV energy absorbed by the grains) heats the gas through photoelectric heating mechanism. The value of ϵ calculated for hydrogen density $N = 10^4$(cm^{-3}) as a function of infrared radiations I_{FIR} (ergs cm^{-2} s^{-1} sr^{-1}) are plotted in Figure 2. From the graph it can be seen that efficiency is maximum for low I_{FIR} which represent a cold and neutral medium. Maximum photoelectric heating

efficiency for WD is ~ 0.029 which is almost same as obtained by Juvela et al. (2003) from HLCs while for BT it is slightly low. Due to increase of FUV radiations more and more grains will be ionized and energy carried by the photoelectrons ($h\nu - I_p$) will be reduced due to positive charge on the grain. Thus heating efficiency decreases with increasing G_0 (increasing I_{FIR} also) and decreasing density.

Line intensities are calculated using the formalism of Qaiyum and Ali (2003) in units of (ergs cm^{-2} s^{-1} sr^{-1}). Calculated intensity ratio of [CII] line emission and FIR (I_{CII}/I_{FIR}) vs I_{FIR} is plotted in Figure 3. In a diffuse medium (low density case) exposed to weak FUV radiation (i.e. low I_{FIR}) the maximum intensity ratio is very close to 2.5×10^{-2} for WD, while for BT it is low. Model calculations are performed to evaluate the intensities I_{CII} and I_{CO} of certain galactic and extragalactic sources of Wolfire et al. (1989) and Crawford et al. (1985). The parameters N (cm^{-3}) (hydrogen density), G_0 and velocity field are varied to obtain the best fit to the observed values of line intensities. Observed and calculated intensity ratios (I_{CII}/I_{CO}) for 11 galactic sources that include HII regions, reflection nebulae, planetary nebulae and bright rimmed molecular clouds as well as six extragalactic sources are plotted in Figure 4. It can be seen from the graph that for both the heating models the calculated values of I_{CII}/I_{FIR} agree well to the observed one. The estimated values of G_0 and N are presented in Table 1. The estimated values of G_0 for WD as well as BT models are remarkably same but electron density differs. Velocity field δV_D of the sources are not listed in the table but it is found to vary in the range $\sim 1-8$ km/sec for the said sources.

3. Interstellar radiation field intensity (G_0) and far infrared emissions

It is a fact that FUV radiation in the energy range $5< h\nu <13.6$ eV is primarily absorbed by dust grain and more than 99% of the absorbed FUV radiation is converted into far-infrared continuum. The remaining (less than 1%) FUV flux is converted into gas phase heating which is reradiated as far-infrared and submillimeter line radiation due to the hyperfine transitions of CII, CI, OI, SiII, FeII and rotational transitions of CO. The remaining interstellar photons with low gas opacity are also absorbed by the dust, and most of the absorbed energy will be radiated in the near- IR and FIR continuum. Hence, integrated FIR emission should be almost equal to the incident FUV integrated intensity (Meixner et al. 1992 and Ingalls et al. 2002). Thus intensity of ISRF which illuminate regions-commonly known as photodissociation regions can be calculated following equations (2-5) of the Appendix. From the equation(3) it is quite clear that integrated FIR emission is propotional to G_0. Hence, observed infrared intensity I_{FIR} may be approximated as:

$$I_{FIR} = CG_0 \tag{1}$$

where C is a constant and it is equal to the slope of I_{FIR} and G_0 curve (Figure 6). Here we take zero intercept assuming that in the absence of ISRF there is no FIR emission. In Figure 6 we have plotted the observed FIR emission intensity I_{FIR} and estimated G_0

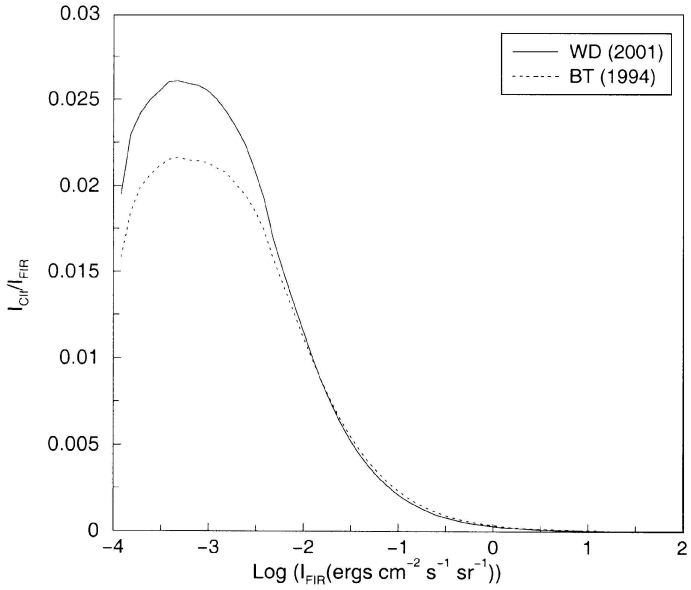

Figure 3. Ratio of [CII] line and far-IR intensities at $N = 10^3$ (cm^{-3}).

from the millimeter and submillimeter line emissions of CII and CO using heating rates of WD. Figure 6 shows that I_{FIR} is linearly dependent of G_0. The slope of the curve is $1.23{\times}10^{-4}$ (ergs cm^{-2} s^{-1} sr^{-1}), which is almost equal to the interstellar radiation field of Habing (1968). This confirms our assumption that all the interstellar radiation field absorbed by the dust is reradiated as FIR emission.

4. Result and discussion

First part of this paper is devoted to a comparative study of the photoelectric heating rates and its efficiency for the models proposed by WD and BT. Further, we study its impact on the thermal, density and velocity structure of photodissociation regions illuminated by FUV radiation field. The FUV radiation field G_0, density N (cm^{-3}) and velocity field δV_D (Doppler velocity) are estimated for photodissociation regions associated with the said galactic and extragalactic sources by comparing the calculated line and observed line intensities of the emissions at mm and submillimeter wavelength from CII and CO. Further more, a relation between FIR emission and G_0 is also established.

Figure 1 shows that for neutral cold medium, where $G_0\sqrt{T}/N_e$ is low WD photoelectric heating rate is higher than that of BT because of contribution to the heating rate from the silicate grains and also grains with a size $a > 10^2$Å. While for the medium where $G_0\sqrt{T}/N_e$ is high, grains are positively charged and the energy carried by the

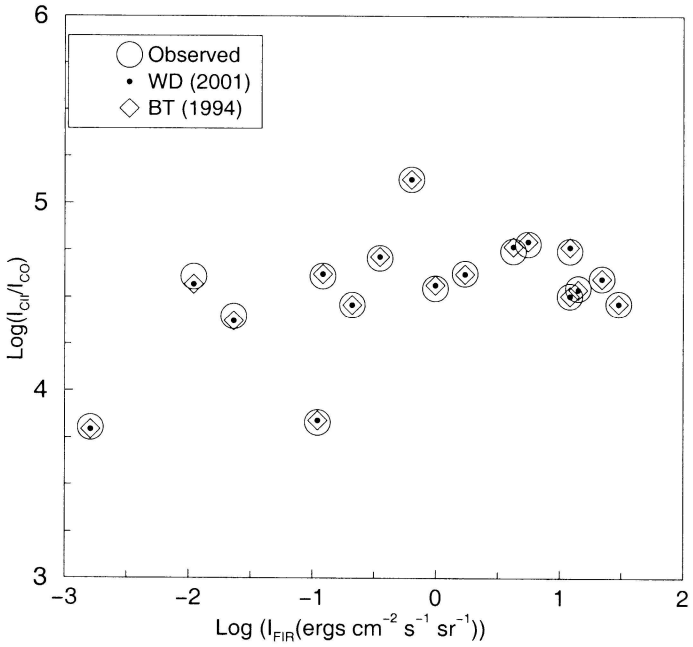

Figure 4. Observed and fitted line intensity ratios [CII] and CO (J=1-0) emissions (I_{CII}/I_{CO}) are plotted against the observed far-IR intensity of the corresponding source.

ejected electrons ($h\nu - I_P$) is decreased resulting in decrease of the photoelectric heating rates. Contrary to the neutral cold medium, photoelectric heating rate in hot and ionized medium is higher for BT than WD due to the large sticking coefficient S_e (which reduces the grain potential I_p) used by BT as compared to WD model. The photoelectric heating efficiency of the gas as a function of continuum FIR intensity is plotted in Figure 2. The maximum heating efficiency is obtained for low I_{FIR} (for small G_0 which ensures cold neutral medium). Surprisingly its maximum value for WD model is $\sim$ 0.029 which is almost same as obtained by Juvala et al. (2003) for HLCs while the same is low for BT. As expected, heating efficiency decreases with the increase of FIR intensity because grains become more and more positively charged and ejected electron carries less and less amount of energy.

Figure 3 represents the fraction of [CII] line emission to integrated continuum FIR emission [I_{CII}/I_{FIR}] as a function of I_{FIR}. In a diffuse medium (low density case) exposed to weak FUV radiation (i.e. low I_{FIR}) the maximum intensity ratio is very close to 2.5×10^{-2} for WD, which is interestingly almost same as observed by Ingalls et al. (2002) for HLCs and further confirmed by Juvela et al. (2003) while for BT it is low. Thus observational facts favour the WD model of heating. Figure 4 displays the observed and calculated intensity ratios for I_{CII}/I_{CO} vs I_{FIR}. Remarkable agreement between

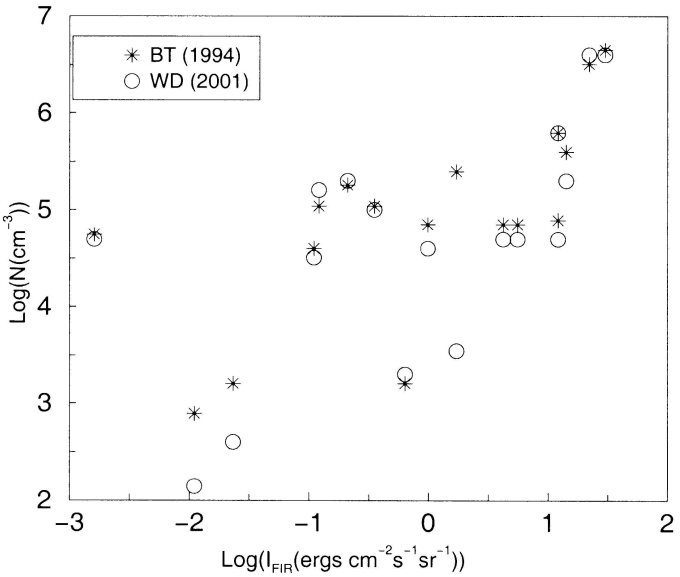

Figure 5. N (cm^{-3}) is the hydrogen density deduced from the intensities of [CII] and CO (J=1-0) using photoelectric heating rates of WD (2001) and BT (1994). N for each source is plotted against the corresponding far-IR line intensity.

observations and calculations are found. The parameters (G_0 and $N(\mathrm{cm}^{-3})$) obtained from the best fit are presented in Table 1. Another parameter, Doppler velocity δV_D, is found varying in the range ∼1-8 km/sec for different sources.

The estimated value of density for each source is plotted as a function of I_{FIR} in Figure 5. It can be seen from the graph that density deduced from the ratio of I_{CII}/I_{CO} differs by a factor $\sim 4-10$ for the models of heating for three sources : M51, M51 HII and NGC 7027 (see Table 1. also). It is worth mentioning here that the best fit of intensity ratio for these three clouds prefers a depleted abundance of carbon $\sim 1.0\times10^{-4}$ as compared to the abundances $\sim 3.0\times10^{-4}$ assumed for other sources. Since electron density in interstellar medium is mostly due to ionization of carbon, therefore, electron density N_e will also be depleted by the same factor. As a result the attachment rate of electron on the surface of charged grain will be reduced. In such a situation $G_0\sqrt{T}/N_e$ will be $> 10^4$, where BT heating rates are enhanced as compared to that of WD. In such circumstances a larger density is required for a balance between heating and cooling to get the calculated intensity ratio to be equal to the observed value. In cases of all other sources the combination of density and G_0 is such that $G_0\sqrt{T}/N_e$ is close to 10^3, where heating rates for said models do not differ significantly as a result density deduced from the intensity ratio are close to each other.

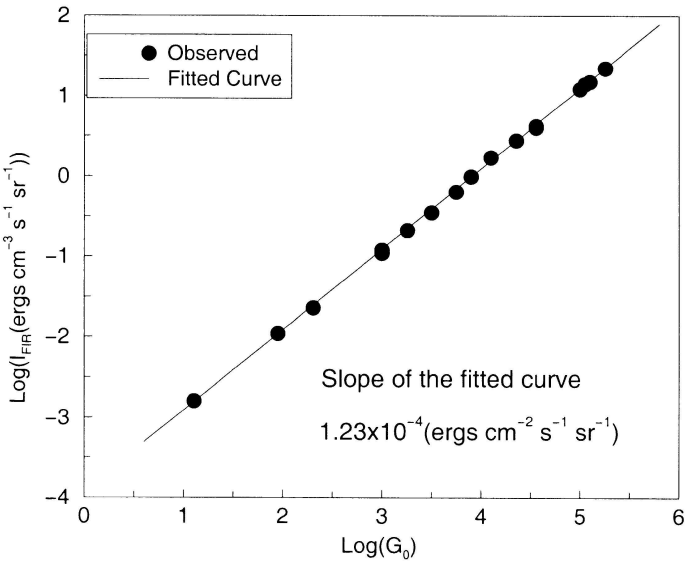

Figure 6. Observed values of far–IR intensity I_{FIR} for different sources are plotted against the estimated values of G_0 from line intensities of [CII] and CO (J=1-0) emissions. The slope of the curve is almost the same as the average ISRF of Habing.

The observed intensity of integrated FIR i.e. I_{FIR} (ergs cm^{-2} s^{-1} sr^{-1}) is plotted against the deduced G_0 in Figure 6. From Figure 6 it can be seen that a linear ralationship exists. A best fit of the I_{FIR} observations and G_0 gives a slope 1.23×10^{-4} (ergs cm^{-2} s^{-1} sr^{-1}) and zero intercept. Interestingly the slope is almost equal to the average interstellar radiation field of Habing (1968). Zero intercept shows that no infrared radiation is possible without interstellar radiation field. Further, it may also be concluded that ISRF photons absorbed by the dust grains are reradiated fully in the near-IR and FIR.

Appendix

The temperature of spherical grain of radius a and material m follows from the photon absorption and emission

$$\pi a^2 \int_0^\infty G_0 F_\nu e^{-K_\nu A_v} Q_{abs,\nu}(a,m) d\nu = 4\pi^2 a^2 \int_0^\infty B_\nu(T_0) Q_{abs,\nu}(a,m) d\nu \qquad (2)$$

where $B_\nu(T_0)$ is the Planck function, T_0 grain temperature and $Q_{abs,\nu}(a,m)$ is the absorption efficiency for the material m and grain size a. $m = 1$ stands for the silicate grain and 2 for carbonaceous grains. $Q_{abs,\nu}(a,m)$ is approximated as $10^{-3}a(\text{Å})$ and $3\times10^{-4}a(\text{Å})$ for carbonaceous and silicate grains respectively for grain sizes of $10\text{Å}\leq a(\text{Å})\leq 1000$ in UV range following WD. The flux of FUV radiation considered here is G_0F_ν where F_ν is

Table 1.

	Source	WD(2001)		BT(1994)	
		G_0	$N(\mathrm{cm}^{-3})$	G_0	$N(\mathrm{cm}^{-3})$
Extra-galactic sources	NGC1068	3.16×10^{3}	1.0×10^{5}	3.16×10^{3}	1.1×10^{5}
	IC342	1.00×10^{3}	1.6×10^{5}	1.00×10^{3}	1.1×10^{5}
	M82	7.94×10^{3}	4.0×10^{4}	7.94×10^{3}	7.1×10^{4}
	M51	1.99×10^{2}	4.0×10^{2}	1.99×10^{2}	1.6×10^{3}
	M51 HII	8.91×10^{1}	1.4×10^{2}	8.91×10^{1}	7.9×10^{2}
	M83	1.00×10^{3}	3.2×10^{4}	1.00×10^{3}	4.0×10^{4}
Galactic sources	M42(Θ^1C)	3.54×10^{4}	5.0×10^{4}	3.54×10^{4}	7.9×10^{4}
	M42(Orion bar)	2.24×10^{4}	5.0×10^{4}	2.24×10^{4}	7.1×10^{4}
	NGC 2023	1.77×10^{3}	2.0×10^{5}	1.77×10^{3}	1.8×10^{5}
	NGC 2024	3.54×10^{4}	5.0×10^{4}	3.54×10^{4}	7.1×10^{4}
	B35	1.26×10^{1}	5.0×10^{4}	1.41×10^{1}	5.6×10^{4}
	Sgr A	1.77×10^{5}	4.0×10^{6}	1.58×10^{5}	3.2×10^{6}
	M17	1.12×10^{5}	2.0×10^{5}	1.12×10^{5}	4.0×10^{5}
	W49N	1.25×10^{5}	4.0×10^{6}	1.25×10^{5}	4.5×10^{6}
	DR21	1.00×10^{5}	6.3×10^{5}	8.91×10^{4}	6.3×10^{5}
	NGC 7027	1.25×10^{4}	3.5×10^{4}	1.25×10^{4}	2.5×10^{5}
	NGC 7023	5.62×10^{3}	2.0×10^{3}	4.46×10^{3}	1.6×10^{3}

due to Habing (1968). By varying the values of G_0 we can take care of radiation field for any cloud of interest. The grain temperature will also vary with the variation of G_0.

Integrating over the grain distribution the dust thermal emission is

$$\Lambda_{d,\nu} = \sum_m \int_{a_{min}}^{a_{max}} B_\nu(T_0) Q_{abs,\nu}(a,m) 4\pi^2 a^{-3.5} da \tag{3}$$

and intensity

$$I_{FIR}(\nu, G_0) = 1.87 \times 10^{21} G_0 \int_0^{A_V} \Lambda_{d,\nu}(A_v) dA_v \tag{4}$$

where

$$dA_v = 0.0015 N dr \tag{5}$$

and N is number density of hydrogen in the photodissociation region and dr is the distance in parsec measured from the surface illuminated by interstellar radiation field. Total integrated intensity may be obtained using equation (4) after considering all the frequencies.

Acknowledgements

The author acknowledges Mr. Badr-e-Alam and Prof. Rahimullah Khan for fruitful discussions and Dr. Tahira Khatoon for her help in reading the manuscript.

References

Bakes, E.L.O., Tielens, A.G.G.M., 1994, *ApJ*, **427**, 822.
Bohlin, R.C., Savage, B.D., Drake, J.F., 1978, *ApJ*, **224**, 132.
Crawford, M.K., Genzel, R., Townes, C.H., Watson, D.M., 1985, *ApJ*, **291**,755.
deJong, T., 1977, *A&A*, **55**, 137.
Draine, B.T., 1978, *ApJS*, **36**, 595.
Habing, H.J., 1968, *Bull. Astr. Inst. Netherlands*, **19**, 421.
Ingalls, J.G., Reach, W., Bania, T.M., 2002, *ApJ*, **579**, 289.
Juvela, M., Padoan, P., Jimenez, R., 2003, *ApJ*, **591**, 258.
Li, A., Draine, B.T., 2001, *ApJ*, **554**, 778.
Meixner, M., Haas, M.R., Tielens, A.G.G.M., Erickson, E.F., Werner, M., 1992, *ApJ*, **390**, 499.
Qaiyum, A., 2003, "Physical and Chemical Processes in Interstellar and Circumstellar Medium" Universal Book House, Aligarh.
Qaiyum, A., Ali, S., 2003, *JAA*, **24**, 69.
Weingartner,J.C., Draine,B.T., 2001, *ApJS*, **134**, 263.
Wolfire, M.G., Hollenbach, D., Tielens, A.G.G.M., 1989, *ApJ*, **344**, 770.